Peer reviewed version

Link to published version (if available):
10.1109/ECCE.2015.7310286

Link to publication record on the Bristol Research Portal
PDF-document

Impact of Slot Shape on Loss and Thermal Behaviour of Open-Slot Modular Stator Windings

Rafal Wrobel, Samuel J. Williamson, Nick Simpson, Sabrina Ayat, Jason Yon, Phil H. Mellor

Department of Electrical & Electronic Engineering

University of Bristol, Bristol, UK

r.wrobel@bristol.ac.uk, s.williamson@bristol.ac.uk, nick.simpson@bristol.ac.uk, sa14034@bristol.ac.uk, jason.yon@bristol.ac.uk, p.h.mellor@brsitol.ac.uk

Abstract— **This paper presents results from an investigation into the optimal design of an open-slot, modular stator winding. The impact of the stator slot shape on the winding temperature rise is explored, taking account the distribution of loss that occurs in the open slot winding, including ac effects, and the heat transfer characteristics from the winding assembly into the stator core pack. The application focus is a single-layer, concentrated wound brushless PM machine, however the work is applicable to other machine formats. Alternative stator lamination profiles are compared; the commonly used parallel sided tooth with a trapezoidal slot, and a parallel sided slot with a trapezoidal tooth. The investigation includes the development of a reduced order thermal model representation of the stator. This model is employed to undertake coupled loss and thermal analyses to provide more accurate comparisons of the designs accounting for ac and temperature effects. The experimental and theoretical findings indicate the parallel sided slot design will result in a 37°C lower winding temperature or an 11% increase in torque at the intended machine operation point.**

Keywords—winding power loss, parallel sided slot design, open-slot modular stator winding, slot shape, thermal analysis;

I. INTRODUCTION

Manufacturability is an important consideration of any electric machine design. This together with the machine's required performance and intended application, is the major driver of initial design choices. 'Design for manufacture' and 'design for performance' therefore represent two, often conflicting, design paradigms. This paper investigates the design of stator assemblies which combine simplicity of manufacture and high-performance. In this context, open-slot, modular stator winding arrangements can provide a number of desirable features. These include high copper fill factor; compact end windings; simplicity and repeatability of manufacture; ease of assembly and superior thermal performance [1], [3]. Performance related drawbacks of open slots include increased torque ripple, elevated winding ac losses and higher rotor losses [11], [12]. These effects are particularly important for, but not limited to, high-performance and compact machine designs.

In high specific output permanent magnet machines, the stator winding assembly is often the dominant source of loss. The stator winding temperature rise ultimately defines the machine output capabilities, and a low-loss stator winding design with improved dissipative heat transfer capabilities would be highly desirable. Limiting the temperature rise between the winding assembly and the stator core pack is particularly challenging, due to the relatively poor conductive thermal properties of readily available electrical insulation system [1]-[6]. There are various impregnation techniques, including high thermal conductivity epoxy resins, which allow for significant improvement in thermal conductivity of the winding assembly [1]-[3]. Compared to the established polymer based varnishes these loaded epoxies tend to be viscous making impregnation difficult, can become brittle under temperature cycling and are not available in the highest temperature classes. Thus if high temperatures and significant mechanical stress or vibration are envisaged during the motor's operation, more established varnished based impregnation systems may be preferred [7].

In principal a winding design that allows for the maximum volume of conductors will have the lowest loss. An open stator slot allows for preformed coils and an excellent conductor fill factor can be realised. However winding ac loss effects cannot be overlooked, and can be particularly problematic with an open slot since the winding conductors are exposed to high levels of leakage flux. Indeed the additional ac losses associated with an inappropriate conductor arrangement can easily overshadow any benefits of a higher conductor fill [8]-[10]. This trade-off between achieving a high volume of conductor at the expense increased ac loss is explored in this paper.

The majority of the stator designs used in low to medium power ac electrical motors are based around a parallel sided tooth, resulting in a trapezoidal slot profile. The approach results in an effective utilisation of the stator core material and suits a winding formed from many stranded circular conductors as is it able to be fitted to the irregular slot profile. The alternative of a parallel sided slot and a trapezoidal shaped tooth can be found in larger distributed wound machines and aircraft generators [14]-[19]. The parallel sided slot is better suited to rectangular profiled conductors and can have superior thermal properties due to close fit of the conductors in the slot. A parallel slot arrangement may be the best choice for an open-slot single-layer concentrated winding as this would allow a simple manufacture and assembly of the preformed coils. The performances of the two alternative slot profiles are compared here in the context of a high fill

preformed winding construction based on rectangular profiled solid conductors and compacted Type-8 Litz wire.

The performance comparisons presented in the paper use numerical finite element electromagnetic analyses to calculate winding loss and a reduced order lumped-parameter thermal equivalent-circuit to estimate the winding temperature rise. The modelling work is calibrated and validated using experimental data taken from tests on full scale 'motorette' sub-assemblies. The outcomes of the comparisons together with details of the modelling approach and the experimental techniques used are provided in the following sections.

II. MACHINE TOPOLOGY AND WINDING CONSTRUCTION

The focus of this research is a relatively low speed high specific torque, air-cooled, radial-flux brushless PM machine. Table I lists the target motor requirements. The targeted continuous specific torque capability exceeds 20Nm/kg, based on the weight of the active stator and rotor elements. In addition to a low overall weight the volumetric envelope of the design was also tightly constrained. A high pole number surface magnet brushless ac permanent topology was selected as being best suited to the application requirements. The choice of 28-24 pole-slot combination allowed for modular single-layer winding arrangement, resulting in a fundamental frequency of approximately 400Hz at the rated operating speed. Fig. 1 presents an outline of the machine active geometry and illustrates some of the key attributes of the selected topology.

TABLE I. TARGET MOTOR REQUIREMENTS

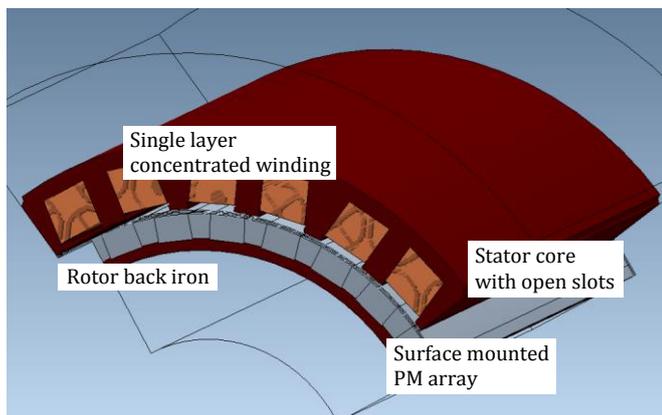| Weight of active materials	50kg
Nominal rotational speed	1700rpm
Nominal power/torque (continuous)	178kW/1kNm
Peak transient power/torque	356kW/2kNm
Target emf at rated speed	110V

Fig. 1. Outline of the PM machine electromagnetic geometry
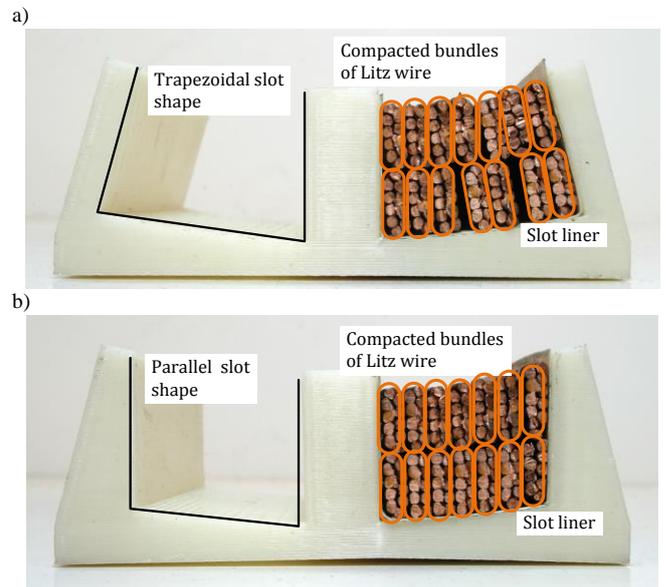

Fig. 2. Rapid prototyped sectors of the stator assembly with compacted Type-8 Litz wire winding conductor option; a) trapezoidal shaped slot geometry, b) parallel sided slot geometry

The open-slot stator lamination greatly simplifies the stator winding manufacture and assembly. The winding coils are performed on a bespoke mandrel and then dropped into the slots. The coils are wrapped in slot liner prior to insertion and a slot wedge is used to secure the coils within the slots, providing electrical insulation and mechanical rigidity. The complete stator assembly is then varnish impregnated and cured. Fig. 2 presents the outcomes of an early trade study into the conductor arrangement and slot shape using rapid prototyped sections to represent the stator tooth and slot structure. To mitigate for ac losses a multi-stranded transposed winding was considered. A compacted rectangular profiled Type-8 Litz construction was selected as it realises a low loss multi-stranded transposed winding with a relatively high conductor fill. This initial investigation clearly shows the parallel sided slot geometry results in a superior conductor lay as compared to the common baseline of a parallel tooth/trapezoidal tooth arrangement, where several cavities are observed between the conductors. This should improve the heat transfer from the preformed winding assembly into the stator core pack. However the parallel sided slot stator core pack is 12% heavier than the baseline solution due to the surplus iron in the tapered teeth.

III. THERMAL MODEL FOR THE SLOT REGION

Thermal analyses were undertaken to quantify the potential benefits of a parallel sided slot and to yield a representative thermal model for the machine. A composite sample representative of the varnish impregnated Type 8 Litz winding was manufactured, Fig. 3, and experimentally characterised using the method described in [26] to obtain equivalent bulk thermal conductivity values for the copper and insulation amalgam of the winding bundle region.
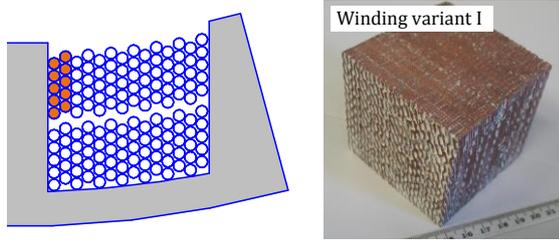
Fig. 3. Outline of the stator slot together with compacted Type-8 Litz wire formed from 10 Ø1.3mm strands; indicated is a single turn within the coil

The thermal measurements on the varnish impregnated winding sample, Table II, demonstrate as would be expected the heat conductivity in the axial orientation of the conductors is much greater than in the plane of the slot. A small degree of anisotropy was also observed in the latter thermal conductivities. 2D finite element (FE) conductive heat flow models were formulated to obtain the temperature profile across the winding and tooth cross section, assuming uniform heat generation in the winding region. Temperature rise and heat flux data from these 2D FEA were used to populate a reduced order lumped parameter thermal model. The use of a reduced order model provides a computationally efficient means of incorporating the interdependence of winding loss with temperature.

Fig. 4 presents the assumed FE model representations of the trapezoidal and rectangular slots. In both cases the same well-formed coil is located in the slot closely fitting to the central tooth shown to the left of the figures. In the case of a trapezoidal slot this results in a void between at the other side of the coil, which is assumed to be filled by air. In line with usual practice the slot sides are lined with a layer of electrical insulating paper. Table II lists the material data used in the FE thermal model.
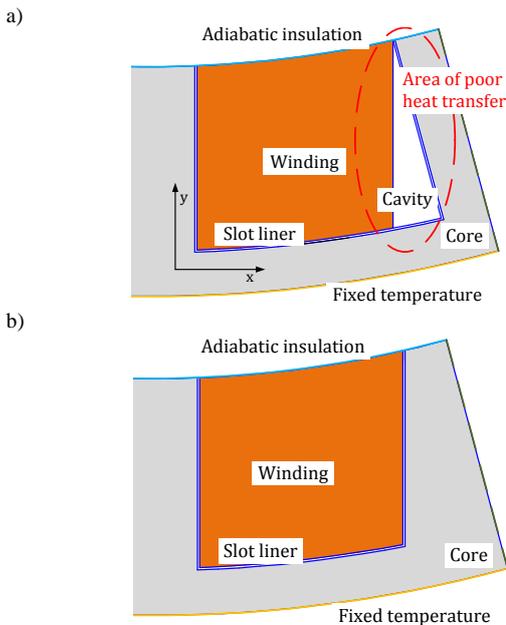

Fig. 4. Thermal model representation of the stator winding assembly together with boundary conditions; a) trapezoidal shaped slot geometry, b) parallel sided slot geometry

TABLE II. THERMAL CONDUCTIVITY DATA ASSUMED IN FE ANALYSIS

Model sub-region	k [W/m·K]
Winding amalgam (circumferential)	1.4
Winding amalgam (radial)	1.7
Winding amalgam (axial)	255
Slot liner	0.14
Stator core	22.0

Fig. 5 illustrates the approach used to extract an equivalent reduced order thermal network for the tooth and slot region from the thermal FEA results. The stator iron is represented as three nodes and the winding region in subdivided into an upper and lower region. The thermal FEA is evaluated at representative levels of heath generation in the winding and tooth regions. The FEA predictions are used to find the average temperature for each of the assumed regions and heat flux across the adjoining region boundaries. Equivalent lumped thermal resistances are then directly calculated from the temperature difference divided by the heat flux.

Table III compares the reduced order network thermal resistance values obtained for the trapezoidal and parallel slot configurations. The values quantify the expected outcomes with parallel slot configuration showing a significantly improved thermal connection to the second tooth (TB). Further the larger section of this tooth in the case of the parallel slot results in a reduced thermal resistance between this tooth and the back iron.

The reduced order thermal network temperatures are easily solved from input of the averaged losses occurring in the lumped regions. The volumetric iron losses were estimated from electromagnetic FEA using the published loss data for lamination material used. The calculation of winding loss, which is temperature dependent, was separated in dc and ac components and is discussed in the next section of the paper.
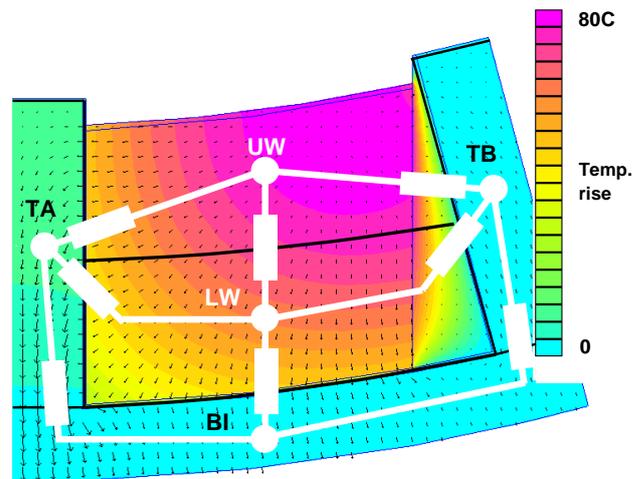

Fig. 5. Equivalent thermal network informed from 2D thermal FEA. The letters denote the lumped thermal region nodes; UW – Upper winding layer, LW-Lower winding layer, TA and TB the Tooth regions and BI the Back Iron.

TABLE III. FEA DERIVED NETWORK THERMAL RESISTANCES

Thermal resistances (Node X to Node Y)	Trapezoidal slot	Parallel slot
UW to LW	1.3 ºC/W	1.1 ºC/W
UW to TA	3.0 (4.3) ºC/W	2.4 (3.7) ºC/W
UW to TB	8.1 (9.4) ºC/W	2.4 (3.7) ºC/W
LW to TA	2.2 (4.5) ºC/W	2.0 (3.2) ºC/W
LW to TB	25 (33) ºC/W	2.0 (3.2) ºC/W
TA to BI	0.9 (1.4) ºC/W	0.8 (1.4) ºC/W
TB to BI	0.46 ºC/W	0.44 ºC/W

Lumped region nodes; UW – Upper winding layer, LW-Lower winding layer, TA and TB the Tooth regions and BI the Back Iron. Corrected values are shown in parenthesis following test calibration of the thermal model

IV. WINDING LOSS MODEL

Whilst dc ohmic losses are relatively easily found from the wire gauge and mean turn length, attention needs to be paid to the winding ac loss effects. Several authors have investigated the causes of ac winding loss [4], [8]-[19]. In addition to eddy current and proximity effects caused by slot leakage fluxes, the ac winding loss from the PM excitation needs to be considered due the open-slot stator topology [11], [17]. In order to derive the ac winding loss a number of 2D electromagnetic FEAs have been conducted. At this stage, the analysis has been limited to modelling a single slot of the stator winding assembly, neglecting any ac effects in the end-winding. Because of the basic symmetry of the single-layer modular winding, the simplified approach of deriving winding power loss has been found sufficient.

The 3D nature of the conductor transposition in the slot active region means an accurate ac winding loss analysis of Type 8 Litz wire is a computationally challenging [20]-[24]. To simplify the analysis ideal conductor transposition is assumed resulting in balanced current share for the individual strands of the Litz bundle. In the case of ideal transposition and where the diameter of the individual conductors is small compared to the skin depth the problem can be viewed as a resistance limited induced voltage driven eddy current effect.
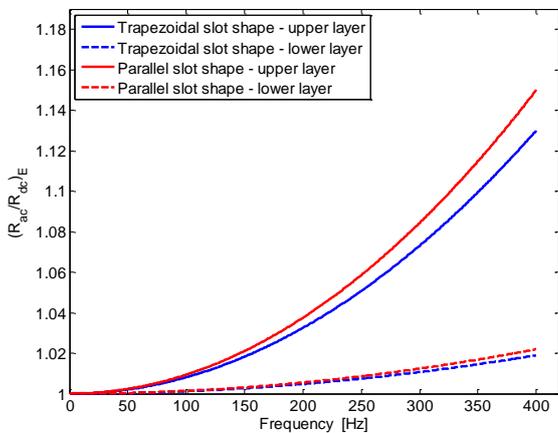
The ac losses will therefore be proportional to the square of the inducing external slot leakage field, the square of frequency and the reciprocal of the equivalent resistance of the eddy current path:

$$P_{ac} \propto \frac{(Bf)^2}{R} = A|_{f_o,T_0} \frac{f^2}{(1 + \alpha(T - T_0))} \qquad , \quad (1)$$

(1) provides insight into how the ac loss of the idealised Litz winding would be expected to vary with frequency and temperature. In principal only a limited electromagnetic FEA would be needed to determine the loss coefficients. The established linear approximation for copper resistivity can be used to scale the FEA predictions to the actual winding temperature, where T_0 is the arbitrary reference temperature of the FEA analyses, T the actual winding temperature obtained from the thermal model and α=0.00393 ºC^{-1}.

Fig. 6 presents the frequency variation of the winding ac loss, calculated using FEA for the upper and lower layers of the Litz winding shown in Fig. 3. The results are presented as an ac loss factor $(R_{ac}/R_{dc})_E$ normalised to the dc value of winding loss. The analyses indicate the majority of the ac loss confined to the upper layer of the winding where the slot leakage fluxes are highest. The magnitude of the ac loss was found to be approximately 15% lower in the case of the trapezoidal slots and is a consequence of the reduced permeance of the larger area slot. The PM rotor induced ac winding loss component was estimated using from FEA to be 180W for full machine at 400Hz operation and is confined to the upper regions of the winding. In order to provide a further degree of confidence to the underpinning design analyses experimental measurements of ac loss were also undertaken on representative stator core and coil subassemblies.

V. EXPERIMENTAL SETUP AND TESTING PROCEDURE

Prior to the construction of the prototype machine full scale sub-assemblies were manufactured and used to validate and calibrate the thermal and ac loss model assumptions. These 'motorettes' comprised a representative stator coil and surrounding tooth structure.

Fig. 6. $(R_{ac}/R_{dc})_E$ vs. frequency for the different winding layers and slot shapes at rated current
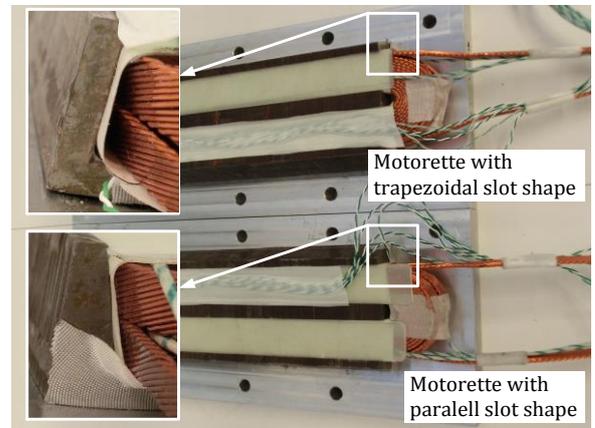

Fig. 7. Instrumented motorette assemblies prior to impregnation; coil with type-8 compacted Litz wire; laminated core pack with M250-35A

The approach allows confidence to be gained in the analyses used to underpin the final machine design in a timely and cost effective way. Details of the experimental setups and testing procedures are outlined in this section.

A. Heat Transfer Analysis

Fig. 7 presents both the trapezoidal and parallel slot motorette assemblies used to validate the thermal model. The pictures are taken prior to varnish impregnation of the sample. The expected cavity between the winding body and slot side is evident for the trapezoidal slot. The windings and insulation system are identical to those of the final coils. The laminated core packs are manufactured from M250-35A silicon iron. To emulate a unidirectional heat flow from the heat source (winding) into the motor housing (heat sink), the motorette body is mounted on a liquid-cooled and temperature controlled 'cold plate' via a profiled aluminium interfacing plate with appropriate retention system. The complete motorette setup is placed in a thermally insulated chamber to emulate adiabatic boundary conditions on the moterette's surfaces, which are not in contact with the cold-plate. The temperature within the motorette assembly is monitored with a number of type-K thermocouples placed in strategic locations including the winding, laminated core pack, aluminium interfacing plate and cold plate.

The test procedure involves connecting the motorette winding to a dc power supply to induce a known value of loss and recording the thermocouple readings after thermal equilibrium is reached. The reference temperature of the 'cold plate' on which the motorette is mounted is maintained constant by a temperature controlled supply of liquid coolant. The measurements were repeated over a range of input powers. Fig. 8 shows the complete experimental setup indicating all the equipment used.
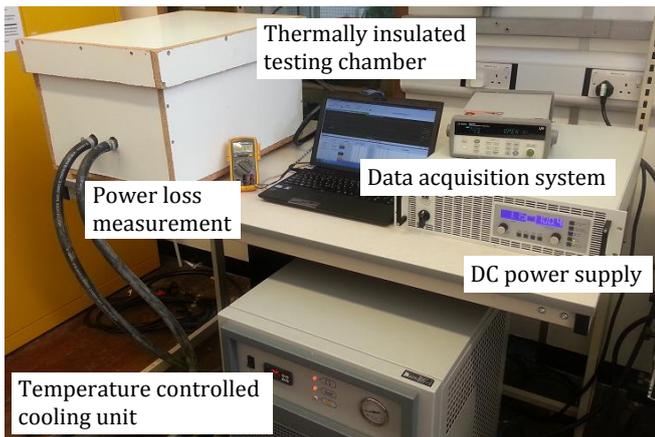

Fig. 8. Experimental setup for motorette dc thermal tests

Fig. 9 presents the winding temperature measured from the motorette assemblies taken over a range injected winding loss. The data is presented as a temperature rise above the stator back iron and is an average of the four thermocouples embedded in motorette winding. The relationship follows the expected linear trend and suggests the experimental setup is

effective in channelling the heat transfer through the test assembly into the cold plate. An equivalent thermal resistance between the winding and core is deduced to be 0.42°C/W and 0.32°C/W for the trapezoidal and parallel sided slots respectively.
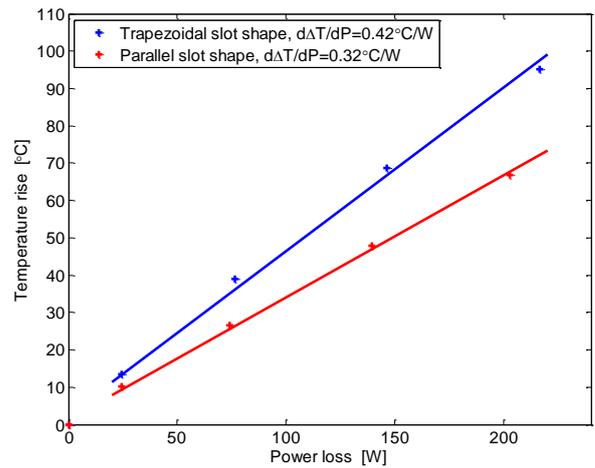

Fig. 9. Winding temperature rise above back iron vs. winding dc power loss

To compare with the test measurements the reduced order thermal model presented earlier was solved for the same conditions as the motorette tests; namely a uniform distribution of loss in the two winding nodes. The model predictions are presented alongside the measurement derived values in Table IV for 200 W loss dissipation in a single coil.

TABLE IV. MEASURED AND MODEL PREDICED WINDING TEMPERATURES (200W LOSS , VALUES REFRENCED TO BACK IRON TEMPERATURE)

	Trapezoidal slot	Parallel slot
Measurement	88 ºC	64 ºC
Initial model - upper winding layer	75 ºC	51 ºC
Initial model - lower winding layer	48 ºC	34 ºC
Calibrated model - upper winding layer	99 ºC	71 ºC
Calibrated model - lower winding layer	73 ºC	54 ºC

As in Fig. 9 the results in Table IV are presented as a temperature rise referenced to the stator back iron. The range of the initial thermal model predictions fell below the measurements, indicating the model is over optimistic in describing the thermal contact between the winding and its surrounding slot. The insertion of the winding conductors in the slot and the subsequent varnish impregnation will not necessarily result in perfect interface between the winding bundle and the surrounding slot liner. Similarly the slot liner will not sit perfectly flush with stator slot sides. The effect is to introduce air voids in the contact with slot liner contact increasing the interface thermal resistance between the winding bundle and slot. It was found that reducing the effective thermal resistance of the slot liner region from 0.14 to 0.058 W/mK resulted in improved model predictions for both the trapezoidal and rectangular slots. The resultant increased thermal contact resistance would be representative of an air cavity of less than a hundred microns at the slot liner

interface. The thermal network resistances were recalculated based on these findings and are shown in parenthesis in Table III. As indicated in Fig. 5 five bulk thermal resistances incorporate the slot liner interface. The calibrated model now yielded estimates of the winding temperature close to the test results, Table IV. Similar accuracy is obtained for the parallel and trapezoidal stator slot geometries. Consequently, it has been concluded that the calibration accounts for manufacture and assembly factors that affect the thermal performance of a practical winding in a similar manner for both slot shapes.

From the experimental and model derived data it is evident that the parallel sided slots would have an improved dissipative capability, as would be expected. The results show a reduction of approximately 35% in the effective thermal resistance between the winding and stator core for the case where the losses in winding are uniformly distributed across its section. As a reduced number of test samples have been used to assess the thermal behaviour of the alternative slot designs, manufacture and assembly factors can affect these findings. However manufacture and assembly issues should manifest equally for the parallel and trapezoidal designs and the observed difference in thermal performance is due to the slot geometry. In the normal operation of an electrical machine the winding losses will not be uniformly distributed across the winding bundle. The resistance of the conductors will change with the temperature profile across the slot. Further individual conductors will be subjected to differing levels of ac loss and these will be highest in the conductors located close to the slot opening. The sensitivity of the considered open slot stator designs to ac loss effects is characterised in the next section.

B. AC Loss Measurements

The extent of the winding ac loss effect can be inferred from a precision impedance measurement. A precision impedance analyser determines an equivalent series resistance for the coil being measured at the test frequency, using which the winding ac loss factor $(R_{ac}/R_{dc})_E$ can be easily derived. Initially a laminated motorette was constructed for this purpose, Fig 10a. Later on in the development cycle the motorette measurements were confirmed through tests on the complete stator assembly, Fig 10b. An attribute of a single-layer modular winding is that each stator coil is electromagnetically decoupled from its neighbour. As a result electrical measurements taken from an individual motorette manufactured in the same manner as the final machine should give similar results to tests on the complete stator assemblies.

Fig. 11 presents the ac loss factor $(R_{ac}/R_{dc})_E$ obtained from complete stator assembly tests. The measurements performed at a room temperature of ~20°C. An insignificant variation between the characteristics of the individual coils was observed indicating a consistent and repeatable coil manufacture. The test derived ac loss effect is around double that indicated from the earlier FEA, Fig. 6. Further whilst the FEA derived value follow the frequency squared relationship expected from (1); the increase in test values ac loss is more linear. The FEA model assumed ideal transposition and
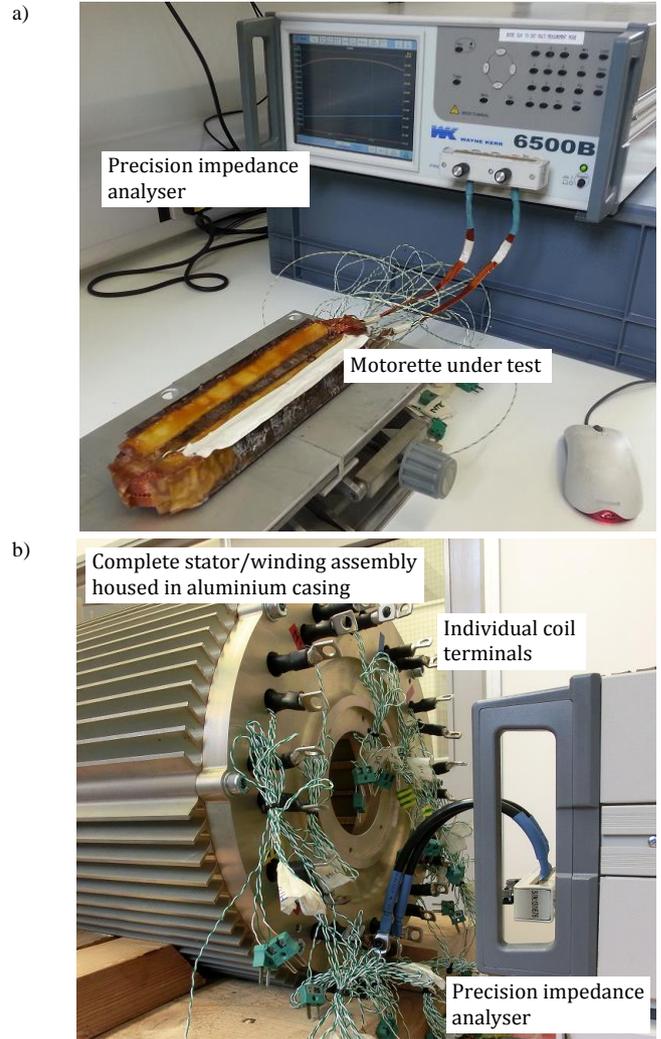
Fig. 10. Experimental setup used to evaluate ac winding loss from armature reaction; a) motorette testing; b) complete stator/winding assembly testing
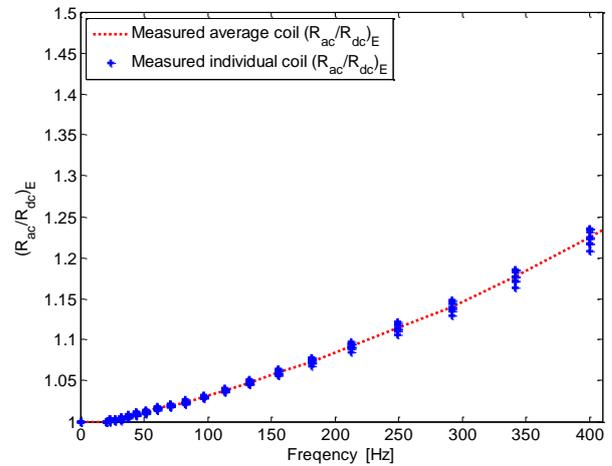
Fig. 11. Measured individual and average per coil $(R_{ac}/R_{dc})_E$ vs. excitation frequency at winding temperature equal to 20°C

current sharing across the parallel conductors making up the Litz winding. In practice the conductor transposition will not be perfect and the resultant bundle effects will introduce additional ac losses.

The ac effects accounted for in the impedance measurements include skin, proximity and circulating current phenomena induced by the stator current. In a permanent magnet machine slot leakage fluxes arising from the passing rotor will induce additional ac loss in the conductors located close to the slot opening. This rotational loss is difficult to quantify by simple experimentation. Whilst a multi-stranded Litz wire with relatively small cross section conductors has been selected to mitigate this effect it cannot be neglected. In subsequent analyses the value of this loss is estimated from a simplified FEA study assuming an ideal transposition of the winding conductors.

VI. Coupled Thermal and Loss Analysis

To provide an insight into how the overall machine performance is affected by the use of particular slot geometry; a thermal analysis of the complete machine was undertaken at the rated operating point using the calibrated reduced order thermal network introduced earlier. The following assumptions were made in regard to the allocation of loss between the two winding layer regions (nodes) in the model:

i) The ohmic (dc) I^2R loss in the conductors is evenly distributed between the upper and lower winding layers. Ohmic loss increase linearly with temperature and scale in accordance to $P_{dc} = P_{dc}|_{T_0}\left(1 + \alpha(T - T_0)\right)$

ii) The ac loss induced by the stator current is distributed between the winding layers in the proportions predicted by the electromagnetic FEA, Fig. 6. The ac losses induced by the passing rotor flux occur only in the upper winding region. The ac losses scale with temperature in accordance to (1) given early in the paper.

iii) All the end windings loss is conducted axially into the slot region and dissipated via the stator core pack. Minimal external cooling of the end windings is assumed. Further it is assumed that ac loss effects in the end windings are negligible.

Table V presents the estimated magnitudes of the loss components corresponding to operation at rated current and frequency. The values given refer to a single slot region catered for by the reduced order model, i.e. are 1/24th of the total stator loss. The loss values are all determined at an arbitrary reference temperature, 20°C and scaled to the actual model estimated winding temperatures using the relationships outlined earlier. Consequently the evaluation of the thermal network required an iterative procedure. At each calculation step the thermal network temperatures are solved and the nodal losses are readjusted to the relevant winding region temperature predictions; the process is then repeated until convergence is achieved. The findings of the thermal analysis are shown in Fig. 12, here the reference case temperature was assumed to be 80°C. The use of the parallel sided slot results

TABLE V. ASSUMED NODAL LOSS BREAKDOWN AT RATED OPERATION (VALUES RELATE TO A SINGLE A SINGLE SLOT REGION AND ARE FOR 20°C)

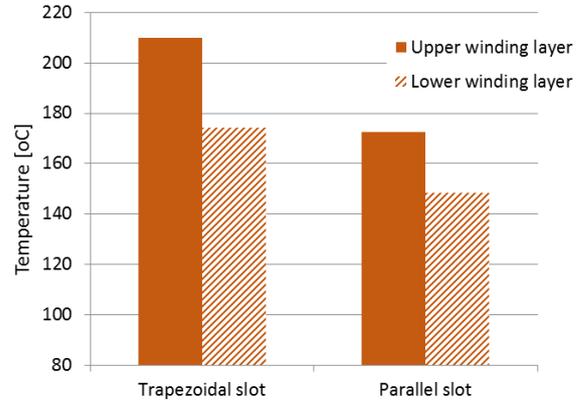| Node and loss type	Trapezoidal slot	Parallel slot
Upper winding layer ohmic losses	32 W	32 W
Upper winding layer ac losses	12.6 W	13.4 W
Lower winding layer ohmic losses	32 W	32 W
Lower winding layer ac losses	Negligible	
Tooth A iron loss	18 W	18 W
Tooth B iron loss	18 W	20 W

Fig. 12. Chart showing predictions from the coupled loss and thermal model

in 37°C lower maximum winding temperature. Further if the trapezoidal slot arrangement was selected the design winding temperature rating (180 °C) would be exceeded. The model was also used to estimate the reduction in the rating of the trapezoidal slot machine design that would be required to yield a similar operating temperature to the parallel slot design. This analysis indicated 11% reduction in the output of the machine at rated speed would be necessary. The penalty of the parallel slot arrangement is a 12% increase in the weight of the stator core pack due to the surplus iron in the tapered tooth. Since the stator core represented around 1/3rd the total active weight of the machine, the use of a parallel slot would give a nett benefit of circa 8% improvement in the output per active weight capability of the machine.

VII. Conclusions

This research has been focused on design considerations of a high-torque-density brushless PM machine. To provide a robust machine construction enabling repeatable manufacture process, an open-slot stator topology with pre-formed winding/coils arrangement has been adopted. Such a construction imposes a number of design challenges some of which include assurance of low power loss and satisfactory dissipative heat transfer to meet the target performance requirements. When making a decision regarding suitable winding design in the context of the open-slot stator topology, it is frequently found that the problem requires in depth understating of the ac winding loss mechanisms and nuances of heat transfer from the winding body into the machine periphery. These two design aspects are the focal points of the paper. To mitigate for the ac loss effects a multi-stranded transposed winding arrangement has been adopted and the

rectangular compacted Type-8 Litz was selected as this maintained an acceptable level of slot fill. However being formed from relatively large diameter conductors the Type-8 Litz construction is not immune to ac loss effects. Conventionally trapezoidal slots are used in machine designs as this makes best use of the iron circuit and provides the largest slot area to accommodate the winding. The open slot concept allows for the use of preformed coils and the rectangular form of the compacted Litz means that the arrangement is more suited to a parallel sided slot. In the analysed case, the parallel slot design provides significant 35% improvement in dissipative heat transfer from the winding body into the stator core pack. However, the improved heat transfer capability for the parallel slot design results in 12% stator core weight increase as compared with the more conventional trapezoidal slot geometry. Taking into account the increase in the mass of the core pack it was concluded the parallel would yield a nett 8% improvement in the output per active weight capability of the machine.

The paper has also presented a methodology for assessing the impact on the choice of slot shape on the overall machine performance. Thermal FEA is used to define a reduced order lumped thermal model for the area of interest. The model is then calibrated against tests on wound sub-assemblies. A similar approach is adopted for quantifying ac loss effects; electromagnetic FEA followed by ac loss measurements on wound sub-assemblies.

REFERENCES

[1] R. Wrobel, P. H. Mellor, "Design Considerations of a Direct Drive Brushless Machine with Concentrated Windings," *IEEE Transactions on Energy Conversion*, vol. 23, no. 1, pp. 1 – 8, March 2008.

[2] R. Wrobel, P. H. Mellor, D. Holliday, "Thermal Modelling of a Segmented Stator Winding Design," *IEEE Transactions on Industry Applications*, vol. 47, no. 5, 2023 – 2030, September – October 2011.

[3] R. Wrobel, P. H. Mellor, N. McNeill, D. A. Staton, "Thermal Performance of an Open-Slot Modular-Wound Machine with External Rotor," *IEEE Transactions on Energy Conversion*, vol. 25, no. 2, pp. 403 – 411, June 2010.

[4] P. Arumugam, T. Hamiti, C. Gerada, "Modeling of Different Winding Configurations for Fault-Tolerant Permanent Magnet Machines to Restrain Interturn Short-Circuit Current," *IEEE Transactions on Energy Conversion*, vol. 27, no. 2, pp. 351 – 361, June 2012.

[5] A. Boglietti, A. Cavagnino, D. Staton, M. Shanel, M. Mueller, and C. Mejuto, "Evolution and modern approaches for thermal analysis of electrical machines," *IEEE Transactions on Industrial Electronics*, vol. 56, no. 3, pp. 871 – 882, March 2009.

[6] D. Staton, A. Boglietti, and A. Cavagnino, "Solving the more difficult aspects of electric motor thermal analysis in small and medium size industrial induction motors," *IEEE Transactions on Energy Conversion*, vol. 20, no. 3, pp. 620 –628, September 2005.

[7] T. Hakamada, Y. Kashiwamura, S. Amagi, "Analysis and Experiments for Thermal Stress of Totally Impregnated Stator Windings," *IEEE Transactions on Electrical Insulation*, vol. EI-18, no. 4, pp. 449 – 454, August 1983.

[8] P. H. Mellor, R. Wrobel, McNeill, "Investigation of Proximity Losses in a High Speed Brushless Permanent Motor," *41st IAS Annual Meeting, IEEE Industry Applications Conference, 2006*, vol. 3, pp. 1514 – 1518, September 2006.

[9] L. J. Wu, Z. Q. Zhu, D. Staton, M. Popescu, D. Hawkins, "Analytical Model of Eddy Current Loss in Windings of Permanent-Magnet Machines Accounting for Load," *IEEE Transactions on Magnetics*, vol. 48, no. 7, pp. 2138 – 2151, July 2012.

[10] Y. Amara, P. Reghem, G. Barakat, "Analytical Predictions of Eddy-Current Loss in Armature Winding of Permanent Magnet Brushless AC Machines," IEEE Transactions on Magnetics, vol. 46, no. 8, pp. 3481 – 3484, August 2010.

[11] R. Wrobel, D. Staton, R. Lock, J. Booker, D. Drury, "Winding Design for Minimum Power Loss and Low-Cost Manufacture in Application to Fixed-Speed PM Generator," *IEEE Transactions on Industry Applications*, pp 1 – 10, May 2015 (*early acess paper*).

[12] R. Wrobel, P. H. Mellor, N. McNeill, D. A. Staton, "Thermal Performance of an Open-Slot Modular-Wound Machine with External Rotor," *IEEE Transactions on Energy Conversion*, vol. 25, no. 2, pp. 403 – 411, June 2010.

[13] X. Wu X., R. Wrobel, P. H. Mellor, C. Zhang, "A Computationally Efficient PM Power Loss Derivation for Surface-Mounted Brushless AC PM Machines," XXI International Conference on Electrical Machines, ICEM 2014, Berlin, Germany, 2-5 September 2014, pp. 17-23.

[14] W. Zhang, T. M. Jahns, "Analytical 2-D Slot Model for Predicting AC Losses in Bar-Wound Machine Windings due to Armature Reaction," *IEEE Transportation Electrification Conference and Expo*, *ITEC 2014*, Dearborn, MI, USA, June 2014, pp. 1-6.

[15] D. A. Gonzalez, D. M. Saban, "Study of the Copper Losses in a HighSpeed Permanent-Magnet Machine with Form-Wound Windings," *IEEE Transactions on Industrial Electronics*, vol. 61, no. 6. Pp. 3038 – 3045, June 2014.

[16] M. Vetuschi, F. Cupertino, "Minimization of Proximity Losses in Electrical Machines with Tooth-Wound Coils," *IEEE Transactions on Industry Applications*, pp. 1 – 9, March 2015 (*early acess paper*).

[17] L. J. Wu, Z. Q. Zhu, "Simplified Analytical Model and Investigation of Open-Circuit AC Winding Loss of Permanent-Magnet Machines," *IEEE Transactions on Industrial Electronics*, vol. 61, no. 9, pp. 4990 – 4999, September 2014.

[18] H. Hamalainen, J. Pyrhonen, J. Nerg, "AC Resistance Factor in OneLayer Form-Wound Winding Used in Rotating Electrical Machines," *IEEE Transactions on Magnetics*, vol. 49, no. 6, pp. 2967 – 2973, June 2013.

[19] P. Mellor, R. Wrobel, N. Simpson, "AC Losses in High Frequency Electrical Machine Windings Formed from Large Section Conductors," *IEEE Energy Conversion Congress and Exposition*, *(ECCE2014)*, Pittsburgh, Pennsylvania, USA, 14-18 September 2014, pp. 5563-5570.

[20] H. Hamalainen, J. Pyrhonen, J. Nerg, and J. Talvitie, "AC resistance factor of Litz-wire winding used in low-voltage high-power generators," *IEEE Trans. Ind. Electron.*, vol. 61, no. 2, pp. 693–700, Feb. 2014.

[21] P. B. Reddy, T. M. Jahns, and T. P. Bohn, "Transposition effects on bundle proximity losses in high-speed PM machines," *in Proc. IEEE ECCE, 2009*, pp. 1919–1926.

[22] J. Acero, R. Alonso, J. M. Burdio, L. A. Barragan, and D. Puyal, "Frequency-dependent resistance in Litz-wire planar windings for domestic induction heating appliances," *IEEE Trans. Power Electron.*, vol. 21, no. 4, pp. 856–866, Jul. 2006.

[23] R. P. Wojda and M. K. Kazimierczuk, "Winding resistance of Litz-wire and multi-strand inductors," *IET Power Electron.*, vol. 5, no. 2, pp. 257–268, Feb. 2012.

[24] S. Wang, M. A. de Rooji, W. G. Odendaal, J. D. van Wyk, and D. Boroyevich, "Reduction of high-frequency conduction losses using a planar Litz structure," *IEEE Trans. Power Electron.*, vol. 20, no. 2, pp. 261–267, Mar. 2005.

[25] P. Mellor, R. Wrobel, D. Salt, A. Griffo, "Experimental and Analytical Determination of Proximity Lossesin a High-Speed Machine," *IEEE Energy Conversion Congress and Exposition*, *(ECCE2013)*, Denver, Colorado, USA, 15-19 September 2013, pp. 3504-3511.

N. Simpson, R. Wrobel, P. H. Mellor, "Estimation of Equivalent Thermal Parameters of Impregnated Electrical Windings," *IEEE Transactions on Industry Applications*, vol. 49, no. 6, pp. 2505 – 2515, November – December 2013.